J Appl Electrochem (2011) 41:1109–1123
DOI 10.1007/s10800-011-0329-5

ORIGINAL PAPER

The occurrence of bromate and perbromate on BDD anodes during electrolysis of aqueous systems containing bromide: first systematic experimental studies

M. E. Henry Bergmann · Tatiana Iourtchouk · Johanna Rollin

Received: 11 February 2011 / Accepted: 27 May 2011 / Published online: 15 June 2011

Abstract Bromide electrolysis was carried out on laboratory-scale cells in the range of 1–1,005 mg [Br^-] dm^{-3} using boron-doped diamond (BDD) anodes. These studies were part of fundamental research activities on drinking water electrolysis for disinfection. Synthetic water systems were mostly used in the experiments, which varied the temperature between 5 and 30 °C, the current density between 50 and 700 A m^{-2}, and the rotation rate of the rotating anode between 100 and 500 rpm (laminar regime). Hypobromite and bromate were found as by-products, as expected. Bromite was not detected. Higher bromate levels were formed at higher current density, but no clear relationship was observed between bromate concentration and the rotation rate or temperatures between 5 and 30 °C. Bromate yields higher than 90% were found at higher charge passed. Perbromate was found as a new potential synthesis or disinfection by-product (DBP), but no perbromate was detected at the lowest bromide concentrations and under drinking water conditions. The perbromate yield was about 1%, and somewhat lower when bromate was used as a starting material instead of bromide. At a temperature of 5 °C more perbromate was detected compared with experiments at 20°. Approximately 20 times more perchlorate was formed compared with perbromate formation in the presence of chloride ions of equimolar concentration. State of mechanistic considerations is presented and a mechanism for perbromate formation is proposed. The reaction from bromate to perbromate was found to be limited that is in contrast to the earlier studied chlorate-to-perchlorate conversion. In the measured concentration range, reduction processes at the mixed oxide cathode showed a much higher impact on the resulting concentration for perbromate than for bromate.

Keywords Electrochemical disinfection · Drinking water · Bromide electrolysis · Bromate · Perbromate · BDD · Disinfection by-products

List of symbols

BDD	Boron Doped Diamond
c	Concentration (mg dm^{-3})
D	Diffusion coefficient (m^2 s^{-1})
DPD	Diphenylendiamine
E	Electrode potential (V (SHE))
F	FARADAY constant (As mol^{-1})
I	Current (A)
IC	Ion chromatography
i_{lim}	Limiting current density (A m^{-2})
k	Reaction rate constant (M^{-1} s^{-1}, M^{-2} s^{-2})
n	Number of electrons transferred
M	Molar mass (mg mol^{-1})
r	Electrode radius (m)
$Re = \omega \cdot r^2/\nu$	Reynolds number
RDE	Rotating disk electrode
RNO	*p*-Nitrosodimethylaniline
rpm	Revolutions per minute
$Sc = \nu/D$	Schmidt number
$Sh = \beta \cdot r/D$	Sherwood number
SHE	Standard Hydrogen Electrode

M. E. H. Bergmann (✉)
Anhalt University, FB 6/7, Bernburger Str. 55,
06366 Koethen, Germany
e-mail: h.bergmann@emw.hs-anhalt.de

T. Iourtchouk
Anhalt University, FB 6, Bernburger Str. 55,
06366 Koethen, Germany

J. Rollin
Anhalt University, FB 7, Bernburger Str. 55,
06366 Koethen, Germany

V	Volume (dm^3)
Δt	Time interval (s)
Δc	Concentration difference (mg dm^{-3})
β	Mass transfer coefficient (m s^{-1})
ν	Kinematic viscosity (m^2 s^{-1})
^{0}dH	Degree of water hardness, still used in Germany. 1^{0}dH is equivalent to 0.1783 mM content of alkaline earth metal ions

1 Introduction

Over the last decade, the number of published papers dealing with water disinfection by direct electrochemical treatment, particularly through flow-through cells, has increased greatly. The process is known under many different brand names, such as *Electrochemical Oxidation*, *Inline Electrolysis*, *Tube Electrolysis*, *Electrochemical Water Activation*, *Electrochemical Sterilization* and *Low-Amperage Electrolysis* [1–5]. Most cells are equipped with electrodes using mixed oxide coatings on Ti carriers. Lately, new electrode materials are suggested [6–9]. Boron-doped diamond (BDD) is a typical representative of these materials, and is known for its high oxidation power and outstanding corrosion resistance [10].

Several research studies have resulted in the discovery of new disinfection by-products (DBPs), such as nitrite [11], ammonium [12], hydrogen peroxide [13], chlorine dioxide [14], chlorite [15], chlorate [16], bromate [17], and perchlorate [16, 18]. The probability of DBP distribution strongly depends on process conditions (water matrix, ionic strength, electrode materials, electrode potential and current density). No definitive predictions can be made. The potential for high chlorate and perchlorate formation was found when electrodes generating radicals (e.g., BDD) were used [19, 20]. Other preliminary experiments [17] showed bromate formation on BDD in the electrolysis of water containing bromide in the range of a few hundred mg dm^{-3}. Although this was outside the concentration limit for drinking water, results permitted the conclusion that bromate would also be found at lower bromide concentration. The German Drinking Water Ordinance (TwVO) and WHO recommendation limits bromate concentration to a maximum of 0.010 mg dm^{-3}. However, the problem is more complex because drinking water is not the only treatment system in practise. Other applications of electrochemical disinfection are the treatment of swimming pool water [21], chiller water and ballast water, for which higher halogenide concentrations are typical. Specifics of DBP formation in *Advanced Oxidation* technologies are discussed more critically in a recent publication [22]. The treatment of wastewater has been the subject of numerous academic studies [23, 24], but is not within the scope of this study.

Normally, bromide is found in drinking water only at very low concentrations. In aquifers close to waterfronts, higher bromide concentrations in the range of a few mg dm^{-3} can be found. Disinfectants containing bromine are widespread in the American market. In ozonation processes, bromide is one reactant for bromate formation [25]. Consequently, bromide concentrations must be monitored. Animal experimentation suggests that bromate may cause kidney cancer. Mechanisms of bromate formation in ozonation processes were presented by von Gunten [26].

Few papers have been published on the effect of bromide electrolysis on anodes generating radicals. Ferro and co-workers studied the kinetics of Br^- and Br_3^- oxidation on Pt [27]. In dealing with BDD anodes, Ferro concluded that bromide oxidation is mass transfer-controlled [28]. Selcuk, on the other hand, studied bromate formation in photocatalysis [29].

This paper is aimed at demonstrating bromate and perbromate formation on BDD in bromide electrolysis. Electrochemical perbromate formation on BDD anodes has been reported for the first time by the authors [30–32], while analysis papers on perbromate formation have been published by Lazarou and co-workers [33, 34]. The new possibilities for perbromate analysis have been reported recently by other authors as well [35]. This paper firstly presents direct determination of perbromate and results of parameter studies for bromate and perbromate formation on BDD anodes in order to stimulate further discussion in the very complicate field. Another goal is to sensitize by-product discussion in electrochemical disinfection, where bromate and perbromate were not known up to now. Due to the high complexity, final clarification of exact electrochemical and chemical mechanisms cannot be within the scope of this publication.

2 Experimental conditions

2.1 Methods and materials

Electrolysis experiments were run on a cell with a rotating BDD anode (in selected experiments it was replaced by a Pt disk electrode), as shown in Fig. 1 and described in [36]. Rotation rate was varied between 100 and 500 rpm as typical for studies in this cell [20]. The circular plate anode had a diameter of 35 mm, and was located 4.5 mm above an expanded mesh cathode of the same diameter (*Magneto Chemie*, molar ratio Ir:Ru = 50%/50%, ratio of active surface to projected surface of 1:1). The anode material (*Condias*) was boron-doped at 2,000–4,000 ppm [20], at a thickness of about 1–2 µm. At this point, it must be

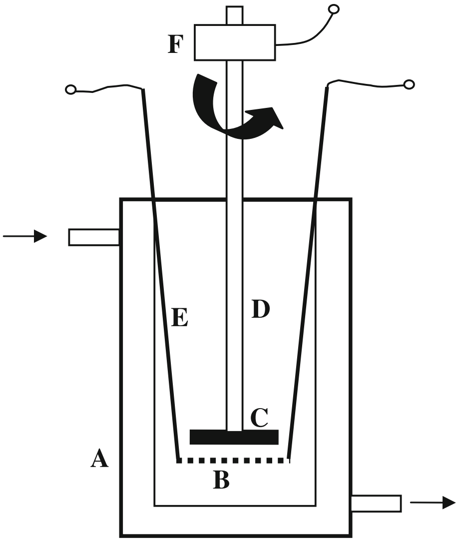

Fig. 1 Electrochemical cell used in the experiments (*A* thermostated baker, *B* expended mesh cathode, *C* BDD anode, *D* rotating shaft, *E* cathodic contacts, *F* rotating contact (*Mercotac*); rotating shaft *D* and cathodic contacts *E* were coated by *Viton* tube material, maximum volume of the cell 160 mL)

emphasized that the use of an undivided cell was the only choice at the present stage of work:

- The undivided cell represents conditions of practical reactors for disinfection purposes.
- The use of separators results in a sudden shift of pH not typical for normal treatment conditions.
- The use of buffers for avoiding pH shift changes mechanisms and product yields because radicals generated at BDD are able to react with buffer constituents added to the water.
- Addition of buffers changes ionic strength of electrolytes.
- Addition of buffers would significantly disturb the highly-sensitive ion chromatography (IC) at µg dm^{-3} level.

Thus, from different points of view, the use of an undivided cell is the only way out despite the fact that products generated anodically may be partially reduced at the cathode. Results presented in Sect. 3.2 show that at least for the bromate, cathodic reduction effects are negligible.

Dissolved NaBr was used as electrolyte in a concentration of a few mmol dm^{-3}. This concentration level leads to measurable reaction effects (for example—reaching bromate concentration maxima at reasonable reaction times or demonstration of reaction competition effects). On the other hand, concentration conditions for IC analysis could be optimized. The volume of electrolyte was usually 100 mL. The cell was an open dark glass beaker thermostated by a *Lauda RM6* cryostat. The constant current mode was adjusted using a *Statron 2252.2* rectifier. The conductivity and pH were measured using *WTW* instruments (*Cond 340i, pH 340*). A current density of up to 200 A m^{-2} was used to minimize the reaction influences of ozone that might be formed at higher current loads. In a few experiments current densities up to 700 A m^{-2} were applied. Samples were taken at different time intervals and were immediately analyzed. Every experiment was performed at least twice. Hypobromite formation was measured using the UV spectrophotometers *Specol 1200* or *Specord 40* (*Analytik Jena*) and DPD test 017 (*Macherey&Nagel, Nanocolor 100D*). Bromate and perbromate were measured by HPLC (see below).

According to a method described by Keil [37] that allows perbromate analysis in the presence of bromate, perbromate was reduced to bromate at boiling temperature and in a solution containing hydrogen carbonate. The iodine that was formed was amperometrically titrated (Eqs. 1–3) at the same temperature with 0.02669N As_2O_3 solution (*Fixanal Riedel-de-Haen* 0.1 g [As] dm^{-1}, 0–50 µA, *Schott Dead-Stop-Titrator TR 151*). The standard deviation of the method is reported as 0.07%.

$$BrO_4^- + 2I^- + H_2O \rightarrow BrO_3^- + I_2 + 2OH^- \quad (1)$$

$$As_2O_3 + 2I_2 + 2H_2O \rightarrow As_2O_5 + 4HI \quad (2)$$

or

$$AsO_3^{3-} + I_2 + 2HCO_3^- \rightarrow AsO_4^- + 2I^- + 2CO_2 + H_2O \quad (3)$$

The titration results obtained could be used for HPLC calibration between 0.010 and 12 mg dm^{-3}.

Polarization curves were studied using an *EG&G* potentiostat model 283 together with a rotating disc electrode stand (model 616) in IR compensation mode. The anode was a 1 cm^2 BDD disc (*Condias*) on niobium. A mercury sulphate reference electrode (*Sensortechnik Meinsberg*, 0.660V vs. SHE) in an outer beaker connected with a salt bridge containing 0.25 M NaOH was used to measure the potential. The cathode was a 15 mm × 30 mm platinum sheet.

2.2 Chemicals

Water for synthetic electrolytes was produced using a *Seralpur Pro 90 CN* deionization unit (conductivity <0.1 µS cm^{-1}). Sodium chloride and sodium bromide (*Sigma-Aldrich*, purity 99.999%), and potassium bromate (*Sigma-Aldrich*, purity >99.8%), were added to deionized water to prepare electrolytes.

The eluent in the HPLC analysis was a mixture of 12 mM *p*-cyanophenol or 4-hydroxybenzonitrile (*Sigma-Aldrich*, purity 95%) with 5 mM LiOH (*Sigma-Aldrich*, purity 99.5%). The suppressor was regenerated using 100 mM nitric acid

(*Merck,* Fixanal 1 M) containing 1% (vol.) acetonitrile (*VWR*, HPLC gradient grade).

XeF_2 of purity higher than 99% (*VWR*) was used in perbromate synthesis.

Iodide and carbonate salt (*Fluka*, analytical grade) were used to adjust neutral pH in amperometric titrations. Perbromate was obtained by electrolysis and by a comparable method using XeF_2 [38, 39]:

$$BrO_3{}^- + XeF_2 + H_2O \rightarrow BrO_4{}^- + Xe + 2HF \quad (4)$$

The HF formed in this reaction was neutralized by 1 M KOH.

Perbromate was synthesized from 3.08 mmol $KBrO_3$ and 3.08 mmol XeF_2, which were added to a 25 mL flask and dissolved in deionised water. An equivalent amount of KOH (6.1 mL) was added for neutralization. A considerable evolution of gas and heat was observed. The pH was checked using a *Unitest* pH test paper and checked against preliminary measurements using a *WTW* pH meter. (The reaction proceeded at pH 8. Because the conversion was not complete, an equivalent amount of KOH was added in order to obtain sufficient high amounts of perbromate.) The detected HPLC peaks were identical to those obtained in electrochemical experiments.

2.3 Perbromate analysis

Perbromate was analysed using HPLC (*Metrohm 761 Compact IC*, *831 Autosampler*, monolithic *Dual* 4-50/4.6 column, precolumn, chemical suppressor, and electrochemical detector). The flow rate was 1.75 mL min^{-1}. The separation by HPLC followed an isocratic method. The injection volume was 1 mL. In most cases, the samples were diluted.

3 Results and discussion

3.1 Bromate formation

3.1.1 Influence of anode rotation rate

Electrochemical bromide oxidation let one expect that products such as bromine and perbromate are formed in a stepwise process controlled at least by bromide diffusion. Form of curves in bromide depletion (not shown here) confirmed diffusion control. An increase in rotation rate from 100 to 300 rpm resulted in a slight increase in bromide depletion rate due to the acceleration of diffusion. At 500 rpm, no further acceleration was observed. The use of a rotating working electrode permits mass transfer estimations to be performed very easily. According to the accepted Levich theory [40], the Sherwood number for a rotating disk electrode can be obtained by solving Eq. 5:

$$\mathrm{Sh} = 0.60 \cdot \mathrm{Sc}^{1/3} \cdot \mathrm{Re}^{1/2} \quad (5)$$

Taking the material data of water and 2.08×10^{-9} m^2 s^{-1} as the diffusion coefficient of the bromide ions, mass transfer coefficients of 3.1×10^{-5}, 5.7×10^{-5} and 7.5×10^{-5} m s^{-1} are obtained for rotation rates of 100, 300 and 500 rpm correspondingly. Equation 6 was used to estimate the limiting current density (e.g., for a concentration of 150 mg $[Br^-]$ dm^{-3} or 1.88 mM, a limiting current of 10.3 A m^{-2} can be obtained at 300 rpm, for $n = 1$).

$$i_{\mathrm{lim}} = n \cdot \mathrm{F} \cdot \beta \cdot c \quad (6)$$

Thus, the system working at 200 A m^{-2} is expected to be under diffusion control [28]. It follows from Eq. 5 that mass transfer is not linearly dependent on rotation rate but rather on the square root. From this we can expect that mass transfer acceleration becomes slower at higher rotation rates.

In addition, one has to expect that the diluted artificial drinking water solution can be under migration control [36]. This would result in larger product formation at higher current density. Thirdly, BDD are probably characterized by radical reaction processes. It has the consequence that a reaction layer inside the diffusion layer is formed that influences on species concentration gradients. So, all calculations have only estimating character. The limiting current density value of 10.3 A m^{-2} mentioned above is coincident with a value of 10.6 A m^{-2} obtained as the maximum reaction rate of $^\bullet$OH radicals with the specific $^\bullet$OH radical scavenger RNO, that was electrolyzed in the same cell at 200 A m^{-2} using 170 mg dm^{-3} sulphate solution as supporting electrolyte [11] (not shown in this paper).

Figure 2 shows the influence of rotation rate on bromate formation. Only slight influence similar to that on the bromide depletion can be seen. Nearly all bromide was converted to bromate toward the end of experiments. This is remarkable because in chloride electrolysis it was found that nearly all chloride was converted to perchlorate [20].

No significant mass transfer acceleration by evolving gases is expected due to several reasons:

(a) At least during the first half of experiments the current at the anode is from reactions without gas evolution.

(b) The action of rising gas bubbles is negligible in comparison with the mass transfer action of the rotating disk electrode (Re = 8,040 at 300 rpm). When for the rotating disk electrode at 300 rpm a Br^- mass transfer coefficient of 5.7×10^{-5} m s^{-1} can be calculated the mass transfer coefficient for gas

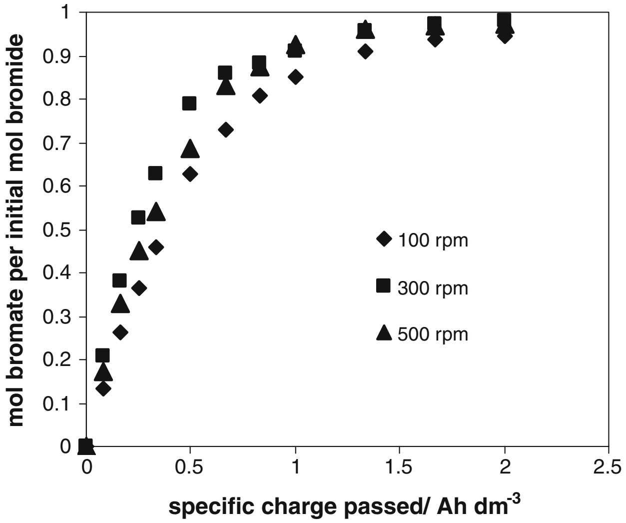

Fig. 2 Bromate yield versus specific charge passed varying rotation rate (BDD anode, IrO_2/RuO_2 cathode, 20 °C, 200 A m^{-2}, 0.1 dm^3, initial bromide concentration: 144–159 mg dm^3 = ca. 1.80–1.99 mM [Br^-], as Na salt)

evolving processes with comparable gas evolving rate at 200 A m^{-2} is in the range of 1×10^{-5} m s^{-1}. Engineering formula [41] show for this relation only very small mass transfer acceleration in the range of a few percent.

(c) The influence of hydrogen on cathodic processes is small in general according to literature data [42].

Figure 3 demonstrates that high differential bromate current efficiency calculated using Eq. 7 may be obtained. It was confirmed in many experiments by obtaining values close to 100% in the beginning of electrolysis.

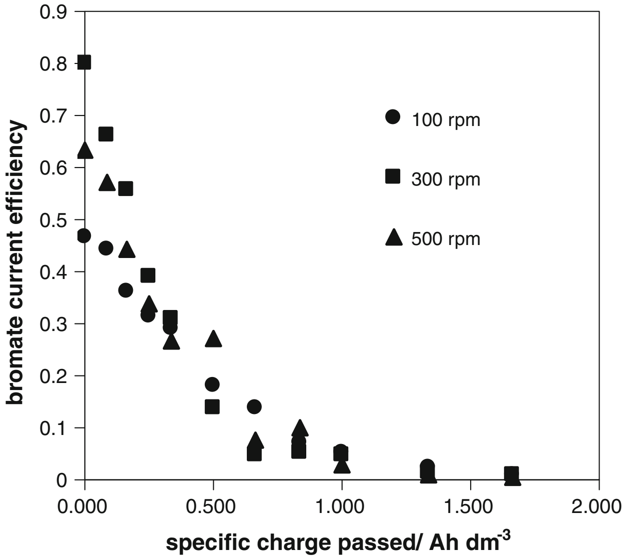

Fig. 3 The differential bromate efficiency versus specific charge passed (BDD anode, IrO_2/RuO_2 cathode, 20 °C, 200 A m^{-2}, 0.1 dm^3, initial bromide concentration: 144–159 mg dm^{-3}, as Na salt)

$$\varphi_{\text{diff}} = \frac{\Delta c \cdot n \cdot \mathrm{F} \cdot V}{\Delta t \cdot I \cdot M} \qquad (7)$$

This behaviour is different to chloride electrolysis when formed chlorine is dissolved to HOCl and Cl^- ion and thus limiting chlorate current efficiency to a maximum of 50%. In case of bromide electrolysis the equilibrium (Eq. 8) is shifted to the left side for low and medium pH [43, 44].

$$Br_2 + H_2O \leftrightarrow HOBr + H^+ + Br^- \qquad (8)$$

Bromine is obviously able quickly to react to bromate without current losses. Table 1 represents an additional example. An earlier work suggests even the action of $O^\bullet$ radicals to explain bromide conversion to bromate at mixed oxide anodes (discussed later in this paper).

Unexpectedly, bromide did not completely convert to bromate even after long experiment times (Fig. 2), indicating the formation of other products. UV spectrophotometry showed the presence of bromine as an expected species [17]. Comparable experiments studying electrochemical chlorate and perchlorate formation from chloride have shown that the mechanism is very complex and has been unknown until today. Thus, explanations of reduced bromate formation are difficult, but reasons for incomplete bromide conversion to bromate can be theoretically discussed:

- Stripping effects by gases formed at the electrodes
- Cathodic reduction reactions
- Anodic oxidation/competing anodic reactions
- Chemical bulk reactions

The phenomena are discussed in the following paragraphs:

- Stripping effects are not very likely at medium and high pH, and low bromine formation rate (see also Sect. 3.1.2).
- Cathodic bromate reduction to bromide is known from industrial bromate production [45] and other studies. The summary reactions are expressed by Eqs. 9 and 10.

  $$BrO_3{}^- + 3H_2O + 6e^- \rightarrow Br^- + 6OH^- \qquad (9)$$

  $$BrO_3{}^- + 2H_2O + 4e^- \rightarrow OBr^- + 4OH^- \qquad (10)$$

  An experiment using only bromate solution as the electrolyte (Fig. 4) really revealed bromide formation. Both change of bromate and bromide reached a steady state-like concentration with time. Taking into account an electron transfer number of 6, average

Table 1 Differential bromate current efficiency during one experiment (initial bromide concentration 288 mg dm^{-3}, 20 °C, 200 A m^{-2}, 0.1 dm^3, 300 rpm)

Specific charge (Ah dm^{-3})	0	10	20	30	40	100	120
Differential current efficiency (%)	99	54	38	30	11	4.4	1.6

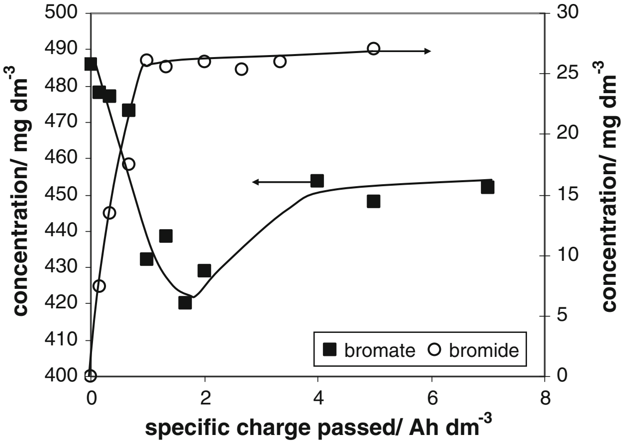

Fig. 4 Bromate and bromide concentration versus specific charge passed (BDD anode, IrO_2/RuO_2 cathode, 300 rpm, 20 °C, 200 A m^{-2}, 0.1 dm^3, initial bromate concentration: 486 mg dm^{-3} = 3.8 mM, as Na salt)

current efficiencies of about 3–5%—both for bromate depletion and bromide formation—could be calculated between 0 and 1 Ah dm^{-3}. This means that cathodic side reactions do not significantly influence on bromate reduction in bromide electrolysis. Indirectly, the fact was already verified in experiments with nearly total bromate conversion (see also Fig. 2 and Sect. 3.1.2). Discussing Fig. 4 it is interesting to note that starting from 1.5 Ah dm^{-3} the bromate concentration grew again in the course of experiment. It is possible that selected anodic reaction become predominant (measurable) only at certain concentration level. So, it is known from chloride oxidation in drinking water that active chlorine, a pre-cursor of chlorate, can be only analytically detected at chloride concentrations higher than approximately 15 mg dm^{-3} [46]. At lower concentration, all chlorine formed is immediately reacted by side products such as H_2O_2. Similar behaviour could be possible for bromide ions and explain the bromate curve in Fig. 4. Furthermore, analysis of Fig. 4 revealed still another interesting fact. Whereas the bromate reduction efficiency in the beginning was about 11% (calculated with Eq. 7, $n = 6$) the bromide formation efficiency was about 9% ($n = 6$). This means a part of bromate was reduced or oxidized into another product.

- Anodic bromate oxidation can be expected in analogy to perchlorate formation [20] and, indeed, by extending bromide oxidation experiments to a longer electrolysis time, a new maximum (later identified as being connected with the perbromate formation) was revealed (see Sect. 3.2). Because high values in bromate yield and bromate current efficiencies can be reached no significant current efficiency for perbromate formation under the given conditions (bromate concentration, current density, temperature) is expected. Compared with non-limited perchlorate formation from chlorate [20] this is again a significant difference.
  Bromate formation in bromide electrolysis is likely very fast and located in a very thin reaction layer near the anode, analogous to chlorate formation on BDD. The effect is known from modelling hydroxyl radical behaviour on BDD anodes [47, 48]: It could be shown that nearly all $^{\bullet}OH$ radicals are consumed in an electrode layer smaller than 1 µm. Therefore, determination of pseudo-kinetic constants and reaction orders as done in other publications dealing with BDD processes was not undertaken in this paper because their results do not explain real mechanisms in the case of very fast chemical conversion under the influence of radicals, which occur in BDD electrolysis. Intensive kinetic studies are necessary for greater clarity. Some mechanistic considerations are given in Sect. 4.
  The first experiments showed that the cell current is distributed between several parallel and consecutive reactions—the oxidation of bromide, formation of bromate and perbromate. Because gas evolution was observed oxygen formation is an additional reaction consuming charge. The $O^{\bullet}$ radical is a probable intermediate in oxygen formation. This fact must be underlined because many effects such as high reaction rates can only be explained by the action of oxygen radicals (Sects. 3.1.4 and 4).
- Bulk reactions are not considered here because kinetic constants of possible reactions are lower by many orders of magnitude compared with probable radical reactions near the electrode.

3.1.2 *Influence of temperature*

The influence of temperature on bromide depletion is very small (not shown here), indicating that temperature had negligible effect on steps involving bromide ions. This behaviour is expected, as bromide reacts in electrochemical reactions according to Eqs. 11–13.

$$Br^- \rightarrow Br^{\bullet} + e^- \tag{11}$$

$$H_2O \rightarrow {}^{\bullet}OH + H^+ + e^- \tag{12}$$

$$Br^- + {}^{\bullet}OH \rightarrow Br^{\bullet} + OH^- \tag{13}$$

Reactions 11 and 12 are electrochemical reactions; reaction 13 is a comparable very fast chemical reaction (reaction constant $k = 1.1 \times 10^9$–1.0×10^{10} M^{-1} s^{-1}). This does not allow expecting any temperature influence on conversion rates. Reaction 11 and 13 may be mass transfer-controlled (see above), but the diffusion coefficients are only slightly temperature-dependent in the considered temperature range. Thus, a temperature increase should have a relatively small influence on bromide reactivity.

Figure 5 shows the influence of temperature on bromate formation yield. (A species yield in the meaning of this paper is defined as the mole number obtained in relation to the initial mole number of bromide.) At lower temperature a slightly decreased bromate formation was observed but at higher specific charge the curve shapes were again quite similar. The effect could not be explained at this stage of work. Volatility effects could not be totally ruled out in a first approach, because bromine vapour pressure increases faster than temperature, but the volatility of bromine solutions is lower than that of chlorine [49]. Comparable chlorine electrolysis under room temperature conditions showed that all chloride may be converted to perchlorate without significant losses in Cl mass balance [20]. Consequently, chemical reaction effects seemed more likely. Moreover, differences can be explained by changes in bromine accumulation if bromine would be formed. Increased perbromate formation would also explain the bromate concentration curves. These facts are in agreement with an understanding of electrolysis as a stepwise oxidation process:

$$\text{Halogenide} \rightarrow \text{active halogen forms} \rightarrow \text{halogenite} \rightarrow \text{halogenate} \rightarrow \text{perhalogenate.}$$

In perchlorate production all these intermediates could be analytically detected. From the steepest slopes of the curves in Fig. 5 the differential current efficiency of bromide oxidation to bromate ($n = 6$) calculated was between 44 and 80%. Besides bromate bromine seems temporarily to be a significant intermediate in the bromide oxidation chain to perbromate. Therefore, bromine concentration was measured in further experiments. It was found that at lowered temperature higher bromine concentration can be measured.

3.1.3 Influence of bromide concentration

One the one hand, higher bromide concentration should increase mass-transfer and the probability of Br^- ion reactions at the anode or near the anodic surface. On the other hand, formation of reactive species may increase reaction competition between bromide ions and these species. The character of normalised concentration curves (Fig. 6) is very similar for the chosen concentrations. Neither pseudo-first order nor pseudo-second order reactions fit the curves (not shown here) because reaction mechanism is complex. The differential bromide current efficiency at the beginning of experiment was in the range between 20 and 25% ($n = 2$, because bromine is obviously the first measurable intermediate; the values are adequate to partial current densities between 40 and 50 A m^{-2}). At higher treatment time, bromide depletion was lower in the experiment using the highest bromide concentration. This is consistent with the assumption of existing competing electrode reactions consuming the supplied charge flow. It is clear that an oxidation process of bromide ions to, finally, bromate ions is characterized by many competing single reaction steps. If for example more charge would be consumed in the reaction of oxidizing bromine and other intermediates less of bromide depletion is expected. In addition, formation of hydrogen peroxide, oxygen and ozone are known as side reactions on BDD anodes in low-concentrated aqueous systems [11]. Furthermore, in Sect. 3.1.4 it is demonstrated that bromide ions depolarise the anode potential whereas bromate ions show opposite behaviour. At the moment, it is not possible to oversee this complicated reaction scheme.

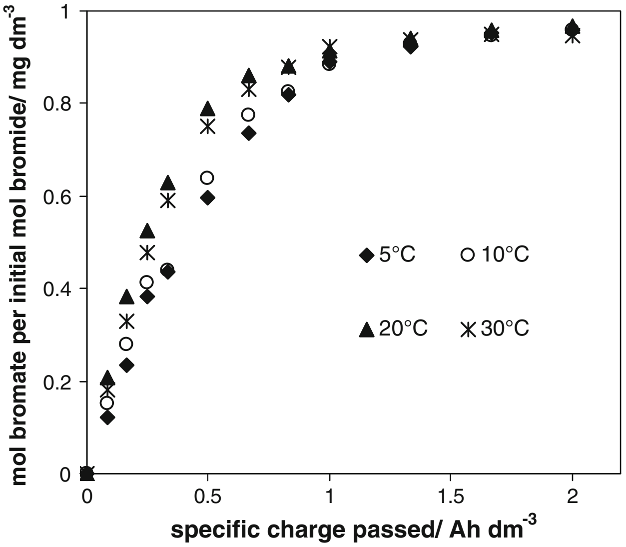

Fig. 5 Bromate yield versus specific charge passed varying electrolysis temperature (BDD anode, IrO_2/RuO_2 cathode, 300 rpm, 200 A m^{-2}, 0.1 dm^3, initial bromide concentration: 144–159 mg dm^{-3} = 1.80–1.99 mM, as Na salt)

Figure 7 includes results of an experiment using higher initial bromide concentration (1,005 mg dm^{-3}). Passed specific charge was increased up to 8 Ah dm^{-3}. Compared with experiments using lower initial bromide concentrations less bromate is formed in the beginning of experiment with 1,005 mg $[Br^-]$ dm^{-3}. The behaviour can be explained by the higher bromine formation. For example, at 0.67 Ah dm^{-3} the bromine concentration was measured as 57 mg dm^{-3} in the 288.8 mg dm^{-3} experiment. For 1,005 mg dm^{-3} approximately three times more bromine was found at the same specific charge passed. It is the logic conclusion that less charge is consumed for the consecutive bromate formation when the summary bromide yield is comparable and nearly 100%.

3.1.4 Influence of anodic current density

The anodic current density was varied between 50 and 200 A m^{-2} in this series of experiments. The mass transfer

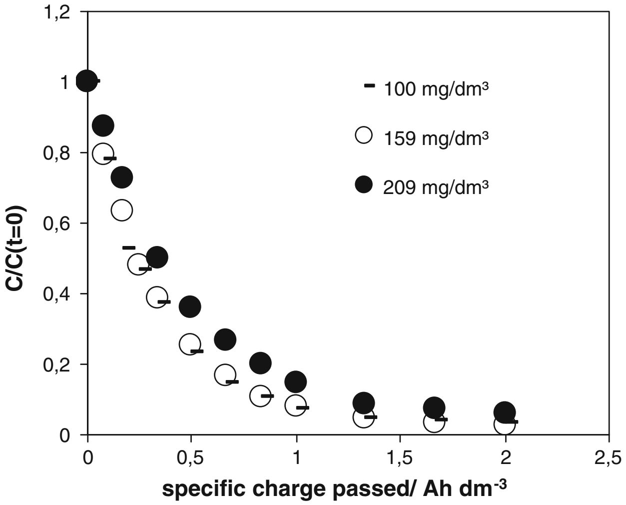

Fig. 6 The influence of bromide concentration in mg dm^{-3} on bromide depletion—normalised bromide concentration (*A*) versus specific charge and negative logarithm of normalised bromide concentration versus treatment time (*B*) (BDD anode, IrO_2/RuO_2 cathode, 300 rpm, 20 °C, 200 A m^{-2}, 0.1 dm^3, as Na salt)

independent limiting current that is often observed in water electrolysis between 10 and 20 A m^{-2}, and that is discussed in terms of limitations for hydroxyl radical transport [50] was exceeded, but ozone generation was still relatively low [20]. Bromide depletion was accelerated by increased current density due to additional migration control. (Diluted systems as treated here may be limited in mass transport both by diffusion and migration [36].) As a consequence of this, more bromate is formed at higher current density (Fig. 8). Detailed discussion is not yet possible because no information on single step reactions exists. Besides migration effects, reactivity effects must be more seriously taken into account. For example, by increasing cell current more O$^{\bullet}$ radicals can be formed and consumed. Although other mechanisms are conceivable for oxygen formation, mechanisms summarized in Eqs. 14–16 are well-accepted.

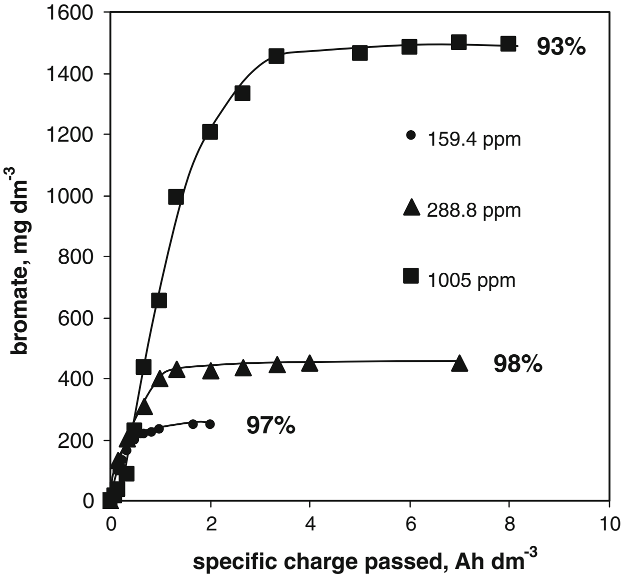

Fig. 7 Bromate and bromide concentration versus specific charge passed (BDD anode, IrO_2/RuO_2 cathode, 300 rpm, 20 °C, 200 A m^{-2}, 0.1 dm^3, varied initial bromate concentration: 159.4, 288.8 and 1,005 mg dm^{-3} = 2, 3.6 and 12.5 mM, as Na salt). The bromide to bromate conversion yield in the end of experiments is indicated in percent

$$^{\bullet}OH \rightarrow O^{\bullet} + H^{+} + e^{-} \tag{14}$$

$$2O^{\bullet} \rightarrow O_2 \tag{15}$$

$$O_2 + O^{\bullet} \rightarrow O_3 \tag{16}$$

Previous polarization studies [11, 20] showed for the electrode material used here, and for a large variety of aqueous systems with ionic strengths comparable to those of drinking waters electrode potentials exceeding 2.5 V (SHE) when current density was chosen at 200 A m^{-2} or higher. For this reason, radical-based mechanisms are highly probable. As one can expect oxygen formation is less intensive at lower current density. In fact, the bromate concentration increases almost linearly at 50 A m^{-2} (Fig. 8). At 100 and 200 A m^{-2} deviations from linearity are observed at much lower charge flow passed showing the beginning diffusion control.

If enough oxygen is available, even ozone formation is observed (Eq. 16), but literature data confirm significant ozone concentrations only for higher current density [51]. Our experiments for determining dissolved ozone concentration using the same electrochemical cell resulted in current efficiencies of about 3% for ozone formation in 170 mg dm^{-3} sulphate solution. This is in agreement with data obtained by Kraft [51]. If present, ozone would be able to participate in relatively slow bromate formation [26], because reaction constants considering reactions with bromide and hypobromite are in the range of 10^2 M^{-1} s^{-1}. Bromine radicals and bromite reacts significantly faster with ozone but bromite (or $HBrO_2$ in the anodic reaction layer) as short-lived intermediates are difficult to analyze [52]. However, if $^{\bullet}OH$ or O$^{\bullet}$ radicals are more easily consumed by other species, lower amounts of oxygen and ozone may be obtained. If reactions 14 and 15 are the main side reactions, nearly no ozone is formed, and all $^{\bullet}OH$ radicals should react with dissolved species or should take part in other reactions to form O$^{\bullet}$, H_2O_2 etc. This can be seen in Fig. 9 in terms of the relatively constant values of differential current efficiency for the lowest current density of 50 A m^{-2}. The higher current efficiency, at increased current densities and at smaller specific charge passed, could be an additional indication of O$^{\bullet}$ radical participation (if other chemical bromate mechanisms are neglected at

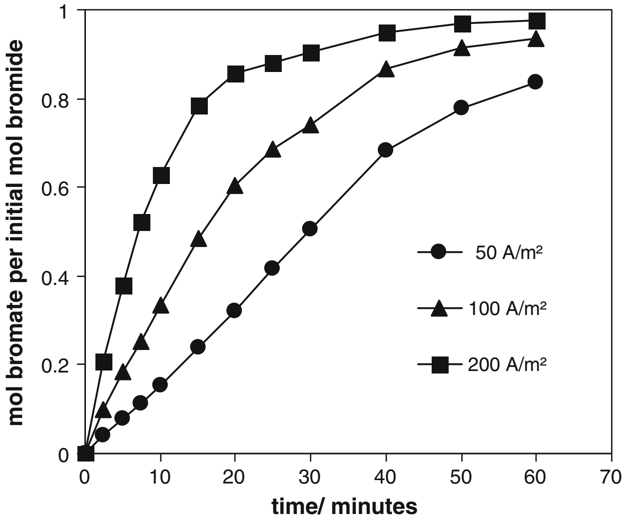

Fig. 8 Bromate formation varying current density (BDD anode, IrO_2/RuO_2 cathode, 300 rpm, 20 °C, 0.1 dm^3, initial bromide concentration: 156–159 mg dm^{-3} = 1.96 mM, as Na salt)

the moment) because concentration of possible radical consumers such as bromine is still high in the initial period of experiment (see Sect. 3.2). For higher charge flow and higher current densities, the differential bromate current efficiency significantly decreases because nearly all bromide and bromine were converted (see Sect. 3.2). Another reason was thought to be the expected formation of perbromate thus lowering bromate concentration. Additional experiments showed, however, that bromate concentration is only remarkably decreasing at relatively high specific charge or at current densities chosen higher than in the experiments described here.

3.2 Perbromate formation

As mentioned above, in selected experiments bromate concentration curves showed maxima versus time or charge flow. A similar behaviour was observed while electrolysing chloride on BDD with the final product of perchlorate [16]. So, it was concluded that formation of perbromate is probable in bromide electrolysis. In parallel, perbromate was synthesized chemically and analysed by titration (see Sect. 2), and the resulting IC was calibrated. Therefore, Fig. 10 is given here because this paper is the first report of direct perbromate determination on BDD. The figure shows a typical chromatogram for a given perbromate concentration. For comparison, one perchlorate peak is given after adding a corresponding amount of ClO_4^- to the solution. Perchlorate and perbromate are clearly distinguishable. In experiments described later, both species were obtained by electrolysing water containing chloride and bromide.

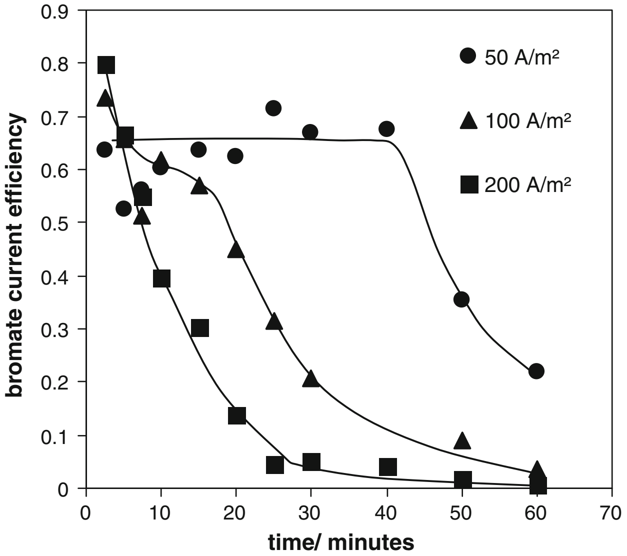

Fig. 9 The differential bromate current efficiency varying current density (BDD anode, IrO_2/RuO_2 cathode, 300 rpm, 20 °C, 0.1 dm^3, initial bromide concentration: 156–159 mg dm^3 = 1.96 mM, as Na salt)

Because bromate was thought to be a precursor of perbromate, the bromate solution was initially electrolysed. Clear perbromate formation was detected (Fig. 11, lower curve). When only a bromide solution at the same starting concentration was electrolysed, more perbromate formation was obtained, although the change in oxidation state was much higher (Fig. 11, upper curve). The influence of counter electrode on cathodic bromate reduction processes can be excluded. To confirm this, experiments were carried out at 200 A m^{-2} replacing the BDD anode by a platinum electrode. It was found that in solutions containing

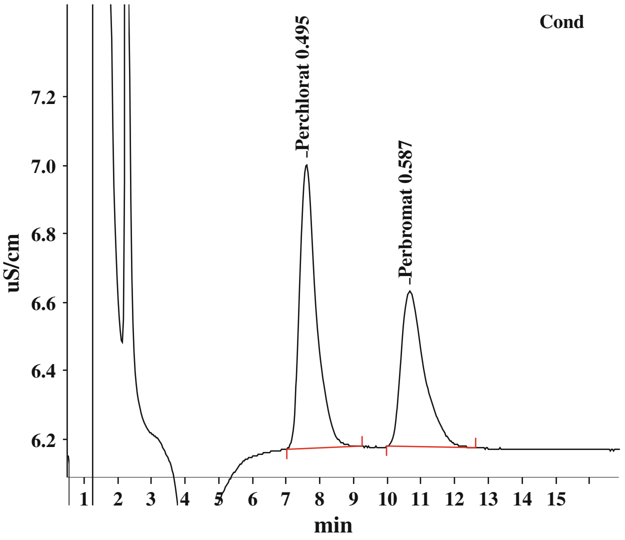

Fig. 10 Chromatograms for perchlorate and perbromate (data in mg dm^{-3})

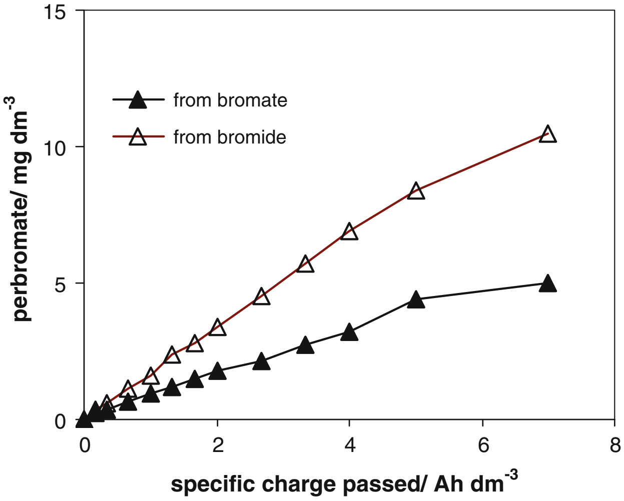

Fig. 11 Perbromate formation from bromide and bromate in single experiments (BDD anode, IrO_2/RuO_2 cathode, 300 rpm, 20 °C, 0.1 dm^3, initial concentration: 3.75 mM, as Na salt)

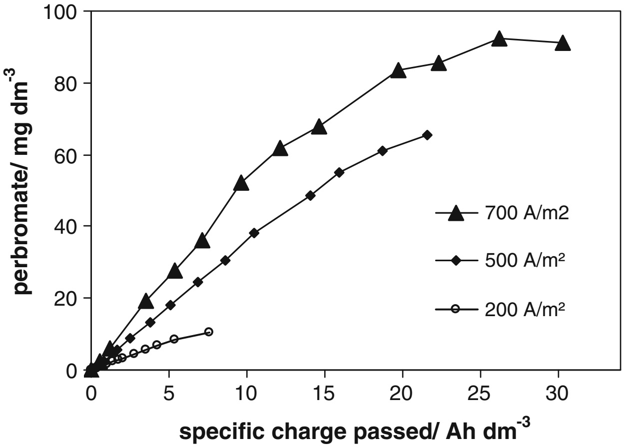

Fig. 12 Perbromate concentration versus specific charge passed varying constant current density (BDD anode, IrO_2/RuO_2 cathode, 300 rpm, 20 °C, 0.1 dm^3, initial concentration: 3.65 mM, as Na salt)

25 mg dm^{-3} (0.17 mM) perbromate, and bromate in the range of 288–1,500 mg dm^{-3} (2.25–11.7 mM) the bromate reduction current efficiency was in the range 0.3–3.3%. Current efficiency for perbromate reduction was lower than 1% in all experiments, i.e. comparable with the data for its formation. Results were validated by mathematical modelling. Nevertheless, because according to Fig. 11 perbromate formation is faster in bromide electrolysis (at 20 °C and 200 A m^{-2}) it can be concluded that in addition to mechanism of converting bromate to perbromate other mechanistic steps, maybe involving bromine and bromite or other species, which are not intermediates in bromate electrolysis, must be taken into account.

For higher current density, higher perbromate concentration was found. Figure 12 compares perbromate formation at three different current densities. At the highest current density a maximum in perbromate formation was found with following reduction characterized by effective current efficiency of 0.12%.

Surprisingly, lower temperature supported perbromate formation (Fig. 13). It means, by applying low temperature perbromate selectivity can be improved.

Higher bromide or bromate concentration did not accelerate perbromate formation (not shown here). More discussion is given in Sect. 4. Suffice it to say here, that electrode reactions on BDD in a solution containing bromate proceed at higher potentials than in bromide containing electrolyte (Fig. 14).

Figure 15 shows the concentration-charge behaviour of those components that could be analysed. Bromite was not found and bromine was formed only temporarily. Bromate was rapidly formed at the beginning. At higher specific charge flow its concentration grew very slowly, because both bromide and bromine were converted to a high extent. In contrast, perbromate concentration grew steadily. The Br balance, in the form of the molar sum of bromide, bromine, bromate and perbromate, was nearly complete, with an average deviation of 2.6% and a maximum deviation from initial Br content of 5.6%. Thus, the probability for the preferred presence of these species containing Br is relatively high. Figure 15 reveals that the rate of bromine formation in the beginning is higher than the rate of bromate formation. At the same time, the rate of perbromate formation is very low and independent on bromine and bromate concentration. It seems that a certain amount of charge and charge carriers is separated for the perbromate formation.

Figure 16 depicts the formation both of perchlorate and perbromate in Cl^-/Br^- electrolysis. The starting molar concentration of chloride and bromide are similar, but the

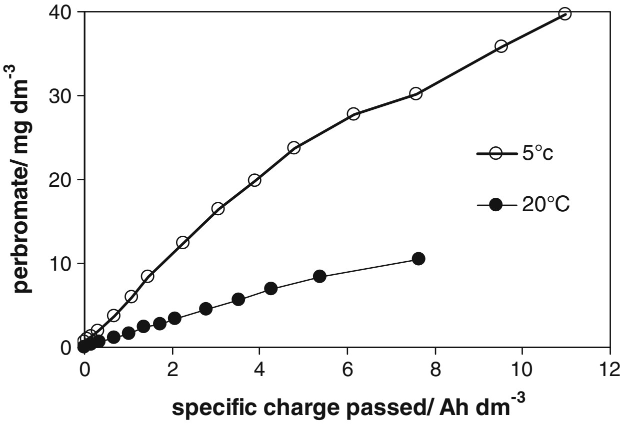

Fig. 13 Perbromate concentration versus specific charge passed varying temperature (BDD anode, IrO_2/RuO_2 cathode, 300 rpm, 20 °C, 0.1 dm^3, initial concentration: 3.65 mM, as Na salt)

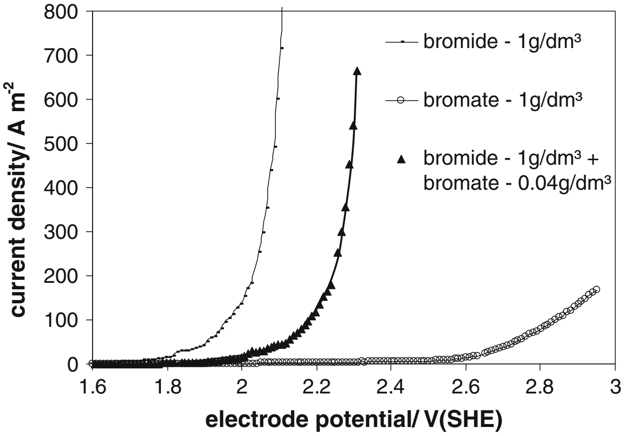

Fig. 14 Anodic polarization curves on rotating BDD anode in different electrolytes (600 rpm, scan rate 50 mV s^{-1}, Pt sheet cathode, 25 °C, saturated mercury sulphate electrode (0.660 V vs. SHE))

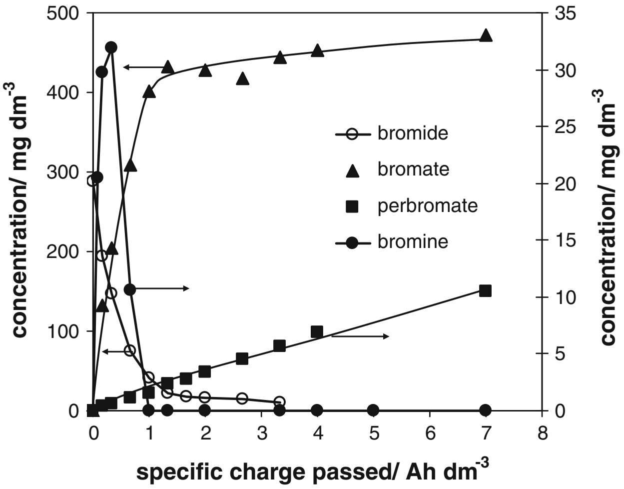

Fig. 15 The concentration of bromide, bromine, bromate and perbromate in bromide electrolysis (BDD anode, IrO_2/RuO_2 cathode, 300 rpm, 20 °C, 0.1 dm^3, initial bromide concentration: 288.8 mg dm^{-3} = 3.6 mM, as Na salt)

formation of perchlorate at the same specific charge flow is preferred. The behaviour is surprising because disinfection chemistry knows chlorine and bromine disappearance in excess chlorine with bromate as a product:

$$2HOCl + 2Br^- \rightarrow 2HOBr + 2Cl^- \quad (17)$$

$$2HOCl + HOBr \rightarrow BrO_3{}^- + 3H^+ + 2Cl^- \quad (18)$$

Chlorate may be a product of chemical interactions between HOCl and HOBr [53]—in dependence on the concentration peculiarities:

$$3HOCl \xrightarrow{HOBr} ClO_3{}^- + 3H^+ + 2Cl^- \quad (19)$$

But reactions 17–19 are not fast enough to compete with radical-bases reactions.

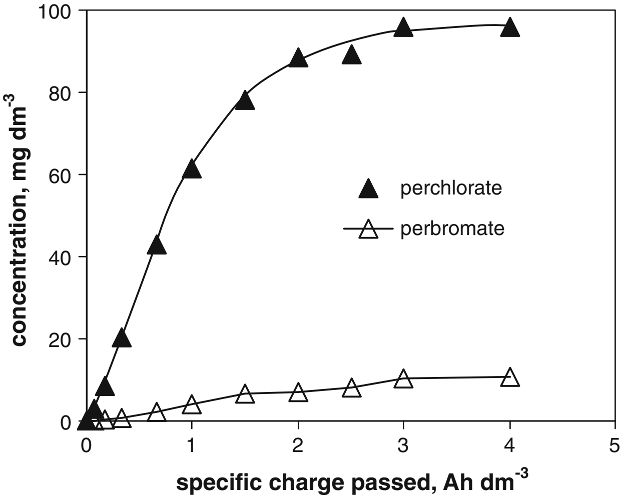

Fig. 16 The formation of perchlorate and perbromate in Cl^-/Br^- electrolysis (BDD anode, IrO_2/RuO_2 cathode, 300 rpm, 20 °C, 0.1 dm^3, initial chloride concentration: 42 mg dm^{-3} = 1.18 mM, initial bromide concentration: 95 mg dm^{-3} = 1.19 mM)

In the first experiments with real water matrices, no perbromate was found. The possible reasons are competing electrochemical reactions or analytical difficulties in overlapping peaks, but further research is necessary.

4 Discussion of possible mechanisms

4.1 The possible role of $^{\bullet}OH$ and $Br^{\bullet}$ radicals

As shown by the confusion over even the first step of halogen ion oxidation, it is still too early to propose a complete mechanism. Under conditions of higher bromide concentration, an electrochemical mechanism is likely for bromide ions [54]:

$$X^- \rightarrow X^{\bullet} + e^- \quad (20)$$

whereas in electrochemistry on mg dm^{-3} and μg dm^{-3} levels with a million-fold excess of water molecules, the direct oxidation by $^{\bullet}OH$ radicals is more realistic at a first step:

$$X^- + {}^{\bullet}OH \rightarrow X^{\bullet} + OH^- \quad (21)$$

Klaening and Wolff [55] found that reaction 20 is (in the case of bromides) a system in which the first intermediate is $BrOH^-$.

$$Br^- + {}^{\bullet}OH \leftrightarrow BrOH^- \quad (22)$$

In the following step, the intermediate reacts to form bromine radical.

$$BrOH^- + H^+ \leftrightarrow Br^{\bullet} + H_2O \quad (23)$$

Formation models for OBr/HOBr from $Br^{\bullet}$ during ozonation are state of knowledge [26]. In case of electrolysis Br_2 formation is possible.

The above mentioned overall side reactions with hydrogen peroxide (or with the HO_2^- ion) are [56]:

$$OBr^- + H_2O_2 \rightarrow Br^- + H_2O + O_2 \quad (24)$$

$$HOBr + HO_2^- \rightarrow Br^- + H_2O + O_2 \quad (25)$$

They may lower the bromine formation efficiency if the bromide concentration is too low for nearly total conversion to bromate that was measured in many of our experiments. Furthermore, bromine is able to form a complex with bromide (Eq. 26)

$$Br_2 + Br^- \leftrightarrow Br_3^- \quad (26)$$

The pK value for this reaction is about 17, i.e. hundredfold higher than for a similar chlorine–chloride complex but for pH higher than 7 it can be totally neglected. In addition, Fig. 15 has shown that bromine only temporarily reveals at relatively low concentration.

It was found in this paper, that partial current densities in selected formation reactions exceed the possible limitation for $^{\bullet}OH$ radicals. One conclusion is the role of chemical reactions, for instance in the formation of bromate. Already Cettou et al. [57] and Pavlovic et al. [58] explained the bromate formation from bromide on RuO_2 anodes by a predominating chemical mechanism (Eqs. 27 and 28).

$$2HBrO + BrO^- \leftrightarrow BrO_3^- + H^+ + 2Br^- \quad (27)$$

$$2BrO^- + HBrO \leftrightarrow BrO_3^- + H^+ + 2Br^- \quad (28)$$

In weakly alkaline media, the reaction rate is relatively slow, with rate constants in the range of 5–16 $M^{-2}\ s^{-2}$ [58]. Kresse, however, found nearly a three times higher bromate formation on BDD anode compared with IrO_2/RuO_2 anode [17]. The most logic conclusion from this is the participation of $^{\bullet}OH$ and $O^{\bullet}$ radicals, whose occurrence is well known.

As discussed above, bromide could be additionally consumed by $^{\bullet}OH$ radical to form $BrOH^-$ and $Br^{\bullet}$ radical. The relatively fast formation and depletion of bromine (Fig. 15) at current densities higher than the limiting current density can yield in an efficient bromate formation that was observed in reality. The mechanism with involvement of $O^{\bullet}$ radicals would be similar to the O_3-based mechanism proposed by von Gunten [56]—with the difference that the highly-reactive O is supplied with higher rate by the anodic process.

von Gunten and Oliveras also explain bromate formation during ozonation using a reaction scheme based on the action of $^{\bullet}OH$ radicals [56]. Intermediates are Br_2^-, Br_3^-, $BrO^{\bullet}$, $HOBr/BrO^-$, BrO_2, BrO_2^-, Br_2O_2. $HOBr/BrO^-$ is a necessary intermediate in bromate formation. Bromate formation reactions are:

$$BrO_2 + {}^{\bullet}OH \rightarrow BrO_3^- + H^+ \quad k = 1.9 \times 10^9\ M^{-1}\ s^{-1} \quad (29)$$

and, less likely:

$$Br_2O_4 + OH^- \rightarrow BrO_3^- + BrO_2^- + H^+ \quad k = 7 \times 10^8\ M^{-1}\ s^{-1} \quad (30)$$

Intermediates were measured by applying radiolysis technology [59, 60]. Reaction constants lie between 10^8 and $10^{10}\ M^{-1}\ s^{-1}$. It is conceivable that similar reactions proceed near the anode surface, where weak physical adsorption of species occurs. Disproportionation of bromine to bromate requires alkaline media and is highly inefficient [56].

4.2 The role of $O^{\bullet}$ radical as a probable reactant

In contrast to the ozonation process, $^{\bullet}OH$ radicals are anodically produced (Eq. 12). If a BDD anode surface is totally covered by reaction species supplied by migration and/or diffusion, hydroxyl radical reactions with them are highly probable. That is the case when organics are electrochemically “incinerated” to CO_2. Drinking water electrolysis conditions are different from this case. At first, reacting species concentration near the electrode is in mM concentration range. At second, distances between active sites seem to be bigger by orders of magnitude compared with mixed oxide anodes. $^{\bullet}OH$ radical diffusion must be considered in three dimensions. Thirdly, reactivity between hydroxyl radicals (Eq. 31) is extremely high with rate constant of approximately $1 \times 10^{10}\ M^{-1}\ s^{-1}$.

$$2^{\bullet}OH \rightarrow H_2O_2 \quad (31)$$

So, hydroxyl radicals generated and diffusing toward solution bulk and along the surface have a high affinity to react between each other or to be reduced to an oxygen radical as typical for higher current densities. Both effects limit the available amount of hydroxyl radicals for chemical reactions with other species. This theory was developed in [48, 50, 61] because polarization studies on the rotating disk electrode showed current densities plateaus independent on rotation rate as mentioned above.

It was concluded that instead of hydroxyl radicals, oxygen radicals are responsible for many reaction effects. Experimentally, the supposition was confirmed when for low ionic strength and high current densities high bromate current efficiencies were measured (Table 1). This does not preclude that a certain amount of hydroxyl radicals take part in chemical or electrochemical species conversion.

Radical chemistry consideration allows reactions schemes, as shown in Eqs. 32 and 32, in this case.

$$O_nX^- + {}^\bullet OH \rightarrow {}^\bullet O_nX + OH^- \quad (32)$$

$$^\bullet O_nX + {}^\bullet OH \rightarrow O_{n+1}X^- + H^+ \quad (33)$$

The idea of $O^\bullet$ radical action is not new. Cettou and coworkers [57] have discussed bromate formation by addition of the $O^\bullet$ radical to the hypobromite ion (Eq. 34)—as a side reaction with main chemical reactions (Eqs. 27 and 28).

$$BrO^- + 2O^\bullet \rightarrow BrO_3{}^- \quad (34)$$

In opposite, it seems that by applying BDD anodes the radical reactions are predominant, with additional chemical side reactions of the Eqs. 27 and 28 type.

O-based chemistry on BDD anodes is accepted in discussions on kinetics [62].

Simple calculations show once more that bromate formation cannot be solely based on $^\bullet$OH radicals. An assumed limiting current density of 15 A m^{-2} for $^\bullet$OH radicals corresponds to an $^\bullet$OH radical generation of 1.55×10^{-7} mol s^{-1}, in our experiments. Calculating bromate production from curve slope in the starting time intervals in Fig. 5, one obtains the value of 1.67×10^{-7} mol s^{-1}, which is the same order of magnitude, but for a six electron transfer mechanism. Logically, not only hydroxyl radicals are responsible for bromate formation, even in its first step of bromide oxidation.

Acceptance of a mechanism as shown in Eq. 34 would postulate the predominating role of $O^\bullet$ radicals at higher current density and explain the high conversion rates.

Unfortunately, at the present stage it is highly-difficult to confirm this by additional experimental methods. Even, distinction between electrochemical steps and fast radical reaction is complicated because both may proceed at similar rates.

The perbromate formation mechanism is still highly speculative. Comparison with perchlorate formation from chlorate let one expect similar kinetic peculiarities [20]. It was found that perchlorate was easily formed, probably by $O^\bullet$ radicals. Starting from equimolar concentration perchlorate formation from chlorate was more favoured than starting from chloride. Figure 11 revealed an opposite effect for bromide and bromate electrolysis. As shown above perbromate formation rate was found extremely low—4.9×10^{-10} mol s^{-1} adequate to a partial current density of 0.1 A m^{-2} and a current efficiency of 0.05% (starting from bromate). This was a surprising result. Obviously, the bromate-to-perbromate reaction is the limiting step in the overall perbromate formation chain starting from bromide. A reasonable explanation was thought to be found when the bromate electrolyte samples (starting concentration 3.8 mM) were analyzed with respect to bromide ions (Fig. 4). Within a few minutes bromide concentration grew to a constant level of 25 mg dm^{-3} (0.3 mM). This concentration is approximately ten times higher than the perbromate concentration when calculated in mole number changes. Bromide is formed from cathodic bromate reduction at relatively low current efficiency as shown above. A probable interpretation of these effects is that

- perbromate formation is bromide-dependent
- additional radicals and reactions have taken into consideration to explain perbromate formation.

But higher bromide concentration did result in better bromine formation but not automatically in enlarged perbromate formation. When bromide concentration in bromide electrolysis was varied between 3.5 and 12.5 mM perbromate formation rate remained unchanged. The behaviour is known from chloride electrolysis because other reactions forming the halogen and halogenate forms are more favoured.

A mechanism that respects both bromide dependence and the extremely low current efficiency could be explained by the presence of bromine radicals (intermediates in bromine formation) and $^\bullet$OH radicals, which are available at low extent:

$$BrO_3{}^- + Br^\bullet \rightarrow BrO_3 + Br^- \quad (35)$$

$$BrO_3 + {}^\bullet OH \rightarrow BrO_4{}^- + H^+ \quad (36)$$

One of these reactions should be very slow whereas the other should have a very high reaction rate for competing with other hydroxyl radical reactions. Possible presence of $Br^\bullet$ radicals was already discussed for explanation of relatively high bromide depletion in Sect. 3.1.2. Kinetic data (reaction constants in the range of 10^5 M^{-1} s^{-1}) give no scope for interpretation concerning an $^\bullet$OH-based oxidation of bromate into the radical form (Eq. 32). Low accessibility of $^\bullet$OH radicals, which would more efficiently react to hydrogen peroxide or with other species in chemical reactions, could also explain an electrochemical perbromate formation scheme according to Eq. 37 [63].

$$BrO_3{}^- + {}^\bullet OH \rightarrow BrO_4{}^- + H^+ + e^- \quad (37)$$

No additional kinetic data are available from literature. Although bromide oxidation to bromate is widely described by von Gunten [26], the author points out that parallel or successive oxidation steps by radicals and ozone may form a nonlinear, unpredictable reaction system. Therefore, a final decision on bromate and perbromate formation cannot be made.

Finally, aspects making discussion still more complicated:

- If additional ions such as nitrate and sulphate are constituents of the water matrix their reactivity has to be proved. For example, nitrate may form radicals, which my react with halogenide ions. The system sulphate/hydrogensulphate act as a radical scavenger [61].

- Electrolysis of solutions, which are poor in ions, produces, especially at higher current density, larger amounts of ozone. In reactions with ozone, short-lived bromite may form bromate.
- Hydrogen peroxide, a by-product in water electrolysis on BDD (Eq. 31), leads to the reduction of HOBr/OBr$^-$ intermediates (see also discussion in Sect. 3.1.2), but usually to a lower extent [56].
- When dissolved oxygen exists in the electrolyte, H_2O_2 may be formed at the cathode, but the formation rate is lower than anodic peroxide formation by one order of magnitude [13], as one may expect some amount of bromine to be reduced to bromide.
- Normally, counter electrode does not have any significant influence on anodic mechanisms. Bromate is only slightly reduced to bromide [this paper and 64]. But in further parameter studies the possible perbromate reduction must be exactly taken into account.
- When hypochlorous acid is present in the solution (for example, from electrolysis of chloride ions following the experimental conditions in Fig. 16) bromate can be chemically formed in a series of relatively slow reactions, as known from disinfection chemistry (Eq. 18) and special studies [65].

5 Summary and conclusions

- Electrolysis of synthetic drinking waters containing bromide ions clearly results in bromate formation on BDD anodes with yields close to 100%. Using bromide concentrations in the mM range resulted in little mass transfer influence, due to limiting reactant conditions and migration control. Higher bromide concentrations and a higher applied current density result in faster bromate formation, though differential bromide current efficiency falls with increasing current density. Temperature decrease to 5 °C does not significantly influence on bromate formation in discontinuous experiments.
- For the first time, on BDD perbromate was directly detected as an additional by-product. Indirectly, results were confirmed in a very recent paper [63]. Consequently, environmentally-oriented applications will have to control both bromate and perbromate concentrations when formation conditions such as the presence of bromide in the mM range and longer treatment time are given.
- The observed effects open prospects for perbromate synthesis by anodic bromide, hypobromite/hypobromous acid or bromate oxidation [30].
- Due to the high complexity of the reaction conditions, the mechanisms of bromate and perbromate formation are difficult to describe. However, comparison with literature data suggest that $^\bullet$OH-based and O$^\bullet$-based mechanisms are highly-probable, with bromine as one of the intermediates and without Br loss by volatility effects. Electrolysis of bromate resulted in constant bromide concentration and extremely slow perbromate formation—two times less efficient than bromide electrolysis at same molar concentration. Partial current density was lower than a theoretical limiting current density for hydroxyl radicals by more than one order of magnitude. Occurrence of different mechanisms for perbromate formation or faster formation of a precursor of perbromate in bromide electrolysis (BrO_3) was concluded. At a temperature of 5 °C more perbromate was formed compared with 20 °C. Because cathodic perbromate reduction is in the same current efficiency range as perbromate formation both chemical effects and temperature effects for cathodic processes can be responsible for the effect. For a current density of 200 A m^{-2} the following "raw" mechanism is proposed:

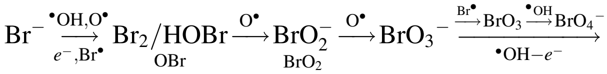

$$Br^- \xrightarrow[e^-,Br^\bullet]{^\bullet OH,O^\bullet} \underset{OBr}{Br_2/HOBr} \xrightarrow{O^\bullet} \underset{BrO_2}{BrO_2^-} \xrightarrow{O^\bullet} BrO_3^- \xrightarrow[^\bullet OH-e^-]{\xrightarrow{Br^\bullet} BrO_3 \xrightarrow{^\bullet OH} BrO_4^-}$$

  There is a limiting step in perbromate formation located between bromate and perbromate.
- Bromine is the only species temporarily detected, in agreement with literature data describing it as a key component for bromate formation in *Advanced Oxidation* processes.
- A comparison of chloride and bromide electrolysis in an undivided cell, at the same molar concentration in solution, shows that the potential of forming perchlorate is much higher than that of forming perbromate—due to mechanistic differences. Experiments in divided cells are not helpful at present due to the fast shifting of pH and kinetic influences from buffer solutions, which would be necessary to keep pH constant.

Acknowledgments The authors wish to thank the German BMBF and AIF/Koeln for project support (KF 1721X04), and Karsten Kresse, Christine Hummel and Dr. Andreas Rittel (Anhalt University) for experimental work. All kinetic constants used in this paper for radical reactions were provided by the Radiation Chemical Data Center.

References

1. Kraft A, Stadelmann M, Blaschke M, Kreysig D, Sandt B, Schroeder F (1999) J Appl Electrochem 29:861

2. Kraft A, Wuensche M, Stadelmann M, Blaschke M (2003) Recent Res Dev Electrochem India 6:27
3. Bergmann H (2008) Drinking water disinfection by direct electrolysis—state of the art. In: CHISA 2008 and 8th European symposium on electrochemical engineering, Prague 24–28 Aug 2008, proceedings, pp 30–46, ISBN 978-80-02-02053-0
4. Kerwick MI, Reddy SM, Chamberlain AHL, Holt DM (2005) Electrochim Acta 50:5270
5. Bergmann MEH (2009) Drinking water disinfection by in-line electrolysis-product and inorganic by-product formation. In: Chen G, Comninellis Ch (eds) Electrochemistry for the environment. Springer, New York, pp 163–205
6. Kraft A, Stadelmann M, Kirstein W (2000) Galvanotechnik 91:334
7. Polcaro AM, Vacca A, Mascia M, Palmas S, Pompei R, Laconi S (2007) Electrochim Acta 52:2595
8. Martinez-Huitle CA, Brillas E (2008) Angew Chem 120:2024
9. Jeong J, Kim C, Yoon J (2009) Water Res 43:895
10. Marselli B, Garcia-Gomez J, Michaud P-A, Rodrigo MA, Comninellis Ch (2003) J Electrochem Soc 150:D79
11. Bergmann H, Iourtchouk T, Borutzky U, Kodym R (2007) Extended studies on mobile water supply systems with enlarged disinfection efficiency (in German). Research report, Anhalt University of Koethen, FKZ 1721X04
12. Michaud P-A, Panniza M, Quattara L, Diaco T, Foti G, Comninellis Ch (2003) J Appl Electrochem 33:151
13. Bergmann H, Koparal AT, Koparal AS, Ehrig F (2008) Microchem J 89:98
14. Bergmann H, Koparal AS (2005) Electrochim Acta 50:5218
15. Bergmann MEH, Schmidt W, Dommaschk A-K (2009) Detection of ClO_2 and ClO_3^- in electrolysed water of very low ionic strength using LGB method and IC. In: Proceedings, annual meting of the international electrochemical society, Beijing (China)
16. Bergmann MEH, Rollin J (2007) Catal Today 124:198
17. Kresse K (2007) Diploma thesis, Anhalt University, Koethen
18. Bergmann H, Rollin J, Czichos C, Roemer D (2007) Labo 26
19. Polcaro AM, Vacca A, Mascia M, Ferrara F (2008) J Appl Electrochem 38:979
20. Bergmann MEH, Rollin J, Iourtchouk T (2009) Electrochim Acta 54:2102
21. Haenni W, Gobet J, Perret A, Pupunat L, Rychen P, Comninellis Ch, Corea B (2002) N Diam Front Carbon Technol 12:83
22. Bergmann MEH, Rollin J, Koparal AS (2010) Chlorate and perchlorate—new criterions for environmentally-friendly processes in *advanced oxidation*. Water Pract Technol (online). doi: 10.2166/wpt.2010.031
23. Alfaro MAQ, Ferro S, Martinez-Huitle CA, Vong YM (2006) J Braz Chem Soc 17:227
24. Martinez-Huitle CA (2007) Mater Res 10:419
25. Schmidt W, Dietrich PG, Böhme U, Brauch HJ (1995) Systematische Untersuchungen zur Bildung von Bromat und bromorganischen Verbindungen bei der Aufbereitung bromidhaltiger Rohwässer in den neuen Bundesländern. Vom Wasser 85:109
26. Gunten Uv (2003) Water Res 37:1469
27. Ferro S, Orsan C, Battisti AD (2005) J Appl Electrochem 35:273
28. Ferro S (2005) J Appl Electrochem 35:279
29. Selcuk H, Sene JJ, Zanoni MVB, Sarikaya HZ, Anderson MA (2004) Chemosphere 54:969
30. Bergmann H, Rollin J, Yurchuk T (2009) German Patent 10 2009 040 651.4
31. Kresse K, Bergmann MEH, Rollin J (2008) Bromate formation on BDD anodes, poster. In: 6th ISE spring meeting, Foz do Iguaçu, Brazil
32. Kresse K, Rollin J, Bergmann H, Hummel C (2008) Electrochemical studies on by-product formation during the electrolysis of waters containing bromide and using mixed oxide and diamond anodes (in Germ.) In: Young Scientists conference, Anhalt University Koethen, book of extended abstracts, pp 27–31, ISBN 978-3-86011-022-5
33. Lazarou LA, Siskos PA, Koupparis MA, Hadjiionnou TP, Appelman EH (1977) Anal Chim Acta 94:475
34. Lazarou LA, Siskos PA, Koupparis MA, Hadjiionnou TP, Appelman EH (1978) Fresenius Z Anal Chem 290:38
35. Megoulas NC, Koupparis MA (2004) Anal Chim Acta 511:159
36. Bergmann MEH, Koparal AS (2005) J Appl Electrochem 35:1321 and Erratum (2006) 36:845
37. Keil R (1976) Z Anal Chem 281:123
38. Appelman EH (1968) J Am Chem Soc 90:1900
39. Appelman EH (1969) Inorg Chem 8:223
40. Levich VG (1962) Physicochemical hydrodynamics, 2nd edn. Prentice-Hall, Englewood Cliffs
41. Vogt H (1978) Electrochim Acta 23:203
42. Janssen LJJ, Barendrecht E (1985) J Appl Electrochem 15:549
43. Liebhafsky HA (1934) J Am Chem Soc 56:1500
44. Beckwith RC, Xiang TW, Margerum DW (1996) Inorg Chem 35:995
45. Zirngiebl E (1993) Introduction to applied electrochemistry (in German). Salle and Sauerlaender, Frankfurt
46. Höll K (ed) (2002) Wasser. de Gruyter, Berlin, p 610
47. Kapalka A (2008) PhD thesis, École Polytechnique Fédérale de Lausanne
48. Bergmann H (2010) Mechanistic consideration of OH radical behaviour on BDD anodes, lecture. In: Annual meeting of the international electrochemical society, Nice (France)
49. William CTI, McCoy F (1990) Hypohalous acid and haloamine flashoff in industrial evaporative cooling systems. Bibliography of technical papers—cooling tower water chemistry, report TP-90-09
50. Bergmann MEH, Iourtchouk, T, Schmidt W, Nüske G, Fischer M (2011) Perchlorate formation in electrochemical water disinfection. In: Perchlorates—production, uses and health effects. Nova Science Publishers, New York (in press)
51. Kraft A, Stadelmann M, Wuensche M, Blaschke M (2006) Electrochem Commun 8:883
52. von Gunten U, Hoigné J (1996) In: Minear RA, Amy GL (eds) Disinfection by-products in water treatment: the chemistry of their formation control. CRC, Boca Raton, p 18
53. Lewin M, Avrahami M (1955) J Am Chem Soc 77:4491
54. Ferro S, De Battisti A, Duo I, Comninellis Ch, Haenni W, Perret AJ (2000) J Electrochem Soc 147:2614
55. Klaenig UK, Wolff T (1985) Ber Bunsenges Phys Chem 89:243
56. von Gunten U, Oliveras Y (1998) Environ Sci Technol 32:63
57. Cettou P, Robertson PM, Ibl N (1984) Electrochim Acta 29:875
58. Pavlovic OZ, Krstajic NV, Spasojevic MD (1988) Surf Coat Technol 37:177
59. Buxton GV, Dainton FS (1968) Proc R Soc A 304:427
60. Buxton GV, Greenstock CL, Helman WP, Ross WP (1988) J Phys Chem Ref Data 17:513
61. Bergmann H (2009) New results of applying diamond electrodes for water hygienization (in German). In: Jahrbuch Oberflächentechnik, Leuze Verlag, Saulgau, pp 317–329
62. Kapalka A, Foti G, Comninellis Ch (2007) Electrochim Acta 53:1954
63. Sáez C, Cañizares P, Sánchez-Carretero A, Rodrigo MA (2010) Electrochemical synthesis of perbromate using conductive-diamond anodes. J Appl Electrochem (online)
64. Badea GE, Badea T (2006) Rev Rom Chem 51:127
65. Huang X, Gao N, Deng Y (2008) J Environ Sci 20:246